Title

Probing Water and Ion Diffusion in Functional Hydrogel Membranes by PFG-NMR

Journal

Macromolecules, 56(12)

ISSN

0024-9297

Authors

Nordness, Oscar
Moon, Joshua D
Marioni, Nico
et al.

Publication Date

2023-06-27

DOI

10.1021/acs.macromol.3c00306

Probing Water and Ion Diffusion in Functional Hydrogel Membranes by PFG-NMR

Oscar Nordness[1,2,3^], Joshua D. Moon[3#^], Nico Marioni[4], Everett S. Zofchak[4], Peter M. Richardson[1,2], Matthew R. Landsman[5,6], Lynn E. Katz[6], Craig J. Hawker[1,7], Venkat Ganesan[4], Rachel A. Segalman[1,2,3], Raphaële J. Clément[1,2*]*

1: Materials Department, University of California, Santa Barbara, CA 93106, United States

2: Materials Research Laboratory, University of California, Santa Barbara, California 93106, United States

3: Department of Chemical Engineering, University of California, Santa Barbara, CA 93106, United States

4: John J. McKetta Jr. Department of Chemical Engineering, The University of Texas at Austin, Austin, TX 78712, United States

5: Advanced Light Source, Lawrence Berkeley National Laboratory, Berkeley, CA , United States

6: Department of Civil, Architectural, and Environmental Engineering, University of Texas at Austin, Austin, TX, United States

7: Department of Chemistry and Biochemistry, University of California, Santa Barbara, CA, 93106, United States

#: Present address: Department of Chemical Engineering, Herbert Wertheim College of Engineering, University of Florida, Gainesville, FL 32611, United States

^Contributed Equally to this work

*Corresponding author

E-mail: rclement@ucsb.edu, segalman@ucsb.edu

ABSTRACT: The effects of ligand basicity on water and ion transport within hydrogel membranes are investigated using a library of functionalizable polyethylene glycol diacrylate (PEGDA) polymer networks with the same crosslink density. Pulsed-Field Gradient NMR characterization of membranes grafted with Lewis base ligands sorbed with a model lithium triflate electrolyte reveals that the self-diffusion of water molecules and ions is primarily driven by the hydration level of the membrane, with ligand functionality playing a secondary role. A comparison of lithium triflate and lithium chloride electrolytes demonstrates greater salt uptake and lower Li^+ and water self-diffusion values for membranes swelled with lithium triflate electrolytes, suggesting that stronger triflate-polymer interactions impede transport within the membrane. These findings are further corroborated by atomistic molecular dynamics simulations that reveal significant coordination between the triflate anion and the polymer, reducing ion and water mobility. These mechanistic insights on the respective roles of membrane hydration and specific-ion effects on transport within ligand-functionalized membranes lay the groundwork for designing high performance membranes for targeted solute separation.

Introduction

Rising global water consumption and increased water scarcity are major societal challenges which necessitates the treatment and subsequent use of nontraditional water resources such as agricultural runoff, waste water effluents, and water produced from hydraulic fracking (i.e., produced water).[1] In order to re-purpose these varied water sources and recover valuable minerals they may contain in an energy and cost effective manner, treatment strategies involving the removal of specific solutes are critical. The recovery and production of fit-for-purpose water from these nontraditional water sources requires the development of next-generation materials capable of solute-tailored separations that are beyond the present capabilities of conventional membranes.[2] Recently, polymeric membranes containing covalently-bonded pendant groups, which can be tuned to selectively coordinate target ions have shown promise for achieving solute-specific separations.[3] The development of such materials is however hindered by a lack of fundamental design rules relating polymer structure and functionalization to solute selectivity and transport.[4] The design of these materials is further impeded by synthetic challenges that make it difficult to isolate the influence of ligand chemistry without significantly altering other polymer network features that also affect solute selective transport.[5]

In a recent study, Moon et al.[6] introduced a modular synthetic platform for accessing a wide library of hydrogel chemistries that leverages active-ester chemistry to enable post-polymerization substitution. Key to this strategy is the preparation of a parent network based on the copolymerization of PEG acrylate and pentafluorophenyl acrylate (PFA) monomers, followed by facile functionalization with a range of amine-containing ligands. Tuning the stoichiometric ratio of the monomers provides direct control over important membrane properties including ligand grafting density, cross-linking density, and the hydration level of the membrane. Moon et

al.'s work investigated the salt sorption properties and permeation behavior of a series of imidazole grafted networks concluding that cation-imidazole interactions may enhance NaCl and LiCl sorption, but are not sufficiently strong to significantly impede monovalent ion diffusion.[6] In the present work, we build upon these findings and explore the effects of membrane chemistry and hydration on microscopic-scale water and ion transport in greater detail.

Traditionally, ion transport in membranes is characterized using macroscopic salt permeation, sorption, and conductivity measurements where average ion self-diffusion coefficients are estimated using the solution-diffusion model.[7-9] In this approach, individual cation and anion self-diffusion coefficients are approximated using the Stokes-Einstein equation in conjunction with predictive thermodynamic models for ion partitioning such as the Donnan/Manning framework introduced by Kamcev et al.[10, 11] While these models have demonstrated good predictive agreement in highly charged and highly swollen membranes, this model generally fails to describe transport in weakly charged or poorly hydrated membranes.[7, 8, 12] Hence, the design of membranes for emerging water treatment applications requires improved predictive models rooted in a molecular-level understanding of the ion-ion, ion-solvent, and ion-polymer interactions underpinning membrane transport properties. These interactions cannot be probed by traditional characterization techniques, calling for the development and implementation of new methods capable of measuring ion and water transport properties separately.

Pulsed Field Gradient (PFG)-NMR is a powerful technique that provides nucleus-specific measurements of self-diffusion coefficients, and can thereby distinguish between cation, anion, and water transport within polymer membranes.[13, 14] Unlike permeation experiments that measure macroscopic transport across the entire membrane, PFG-NMR probes transport on the micrometer scale, offering critical insights into local ion and water dynamics within the membrane.

Unfortunately, many traditional ions of interest (e.g. Na^+ and Cl^-) consist of nuclei that are subject to rapid NMR signal attenuation, which has limited the application of PFG-NMR techniques for characterizing membrane transport. To overcome these limitations, we investigate membrane samples sorbed with an aqueous lithium triflate (LiOTf) electrolyte. The utility of aqueous LiOTf is derived from the presence of multiple NMR-active nuclei, which allows for the determination of water, lithium, and triflate self-diffusion coefficient on the same system through ^1H, ^7Li, and ^{19}F PFG-NMR experiments, respectively. We complement these measurements with atomistic molecular dynamics (MD) simulations to develop a comprehensive, molecular-level understanding of the role of ion-polymer interactions in water and ion transport within these hydrogel-based membrane systems.

In this work, we leverage a versatile polymer backbone chemistry to probe the isolated effects of ligand chemistry (i.e., Lewis basicity) and membrane hydrophobicity on the water uptake, solute sorption, and microscopic water and ion transport in ligand-functionalized hydrogel membranes. The experimental measurements and MD simulations presented herein reveal that ion transport is primarily governed by membrane hydration level, while ligand identity plays a lesser role. At the same time, comparison of lithium triflate (LiOTf)- and lithium chloride (LiCl)- sorbed membranes demonstrates that anion identity influences both salt sorption and transport, with LiOTf demonstrating greater salt sorption coupled with slower water and ion self-diffusion values. These findings provide important mechanistic insights towards the design of next-generation membranes for solute-targeted separations.

Materials and Synthesis

Polyethylene glycol diacrylate (PEGDA, 700 g/mol), polyethylene glycol methyl ether acrylate (PEGMEA, 480 g/mol), butyl acrylate (BA), and 4-(aminomethyl)piperidine (96%) were

purchased from Sigma Aldrich and used as received. 4-(2-aminoethyl)pyridine) (≥97.0%) was purchased from TCI and used as received. 1-(3-aminopropyl)imidazole (APIM) (98%) was purchased from Alfa Aesar and purified by passing once through basic alumina. Pentafluorophenyl acrylate (PFPA) was synthesized using previously reported methods.[6] Polymer networks were prepared using solvent-free, UV-initiated free-radical polymerization based on PEGDA/PEGMEA procedures described previously.[15, 16] Monomer mixtures were prepared by dissolving 0.1 wt% DMPA photoinitiator in a solvent-free mixture of PEGDA, PFPA, PEGMEA, and BA co-monomers. Mixtures were cast between two quartz plates spaced 400 μm apart and polymerized using 365 nm UV irradiation at a power density of ~2 mW/cm^2. Complete crosslinking was achieved after 90 seconds of irradiation, with subsequent dialysis in tetrahydrofuran (THF) revealing sample gel fractions between 96-98%. Post-polymerization substitution of the tethered pentafluorophenyl ester groups was completed by soaking the membranes at room temperature for 24 hours in solutions prepared with (5 wt%) amine in THF (95wt%). The membranes were soaked in sufficient quantities of the 5/95 wt% amine/THF solutions in order to ensure a large excess of amine was present relative to the number of pentafluorophenyl ester groups. As described in our previous work[6] this synthetic protocol achieves quantitative PFPA conversion to the amide. In the present study, FTIR further verified complete conversion of the active esters and did not detect any residual PFPA (e.g., C-F stretches). Samples were subsequently purified by soaking overnight in 0.1 M HCl followed by dialysis with deionized water, exchanging multiple times.

Experimental

Ligand pK_a Measurements

Potentiometric titrations were performed to determine the effective acid dissociation constants (pK_a) of the ligand-functionalized membranes. First, membrane discs (5 mm diameter, 500 µm

thick) were dried under vacuum for 24 h and transferred to a nitrogen glovebox. During the glovebox transfer, membranes were stored under vacuum for 30 minutes to remove residual CO_2. In an inert atmosphere, membranes were hydrated in 5 mL of 0.1 M NaCl for 48 h and solution pH was measured using a combination electrode (Orion 8103BNUWP, Thermo Scientific); the measured pH was assumed to be a direct reading of the hydrogen ion activity. All solutions were purged with nitrogen gas prior to transferring them to the glovebox. Following equilibrium, a small amount (10-30 μL) of acid/base, which included 0.02 M hydrochloric acid and 0.02 M sodium hydroxide (standardized using potassium hydrogen phthalate), was added to the vials and solution pH was recorded. This process was completed every 48 h for six replicates until a full titration curve was obtained for each of the ligand-functionalized membranes. The pK_a values were determined by fitting the titration data to theoretical titration curves via a nonlinear least-squares regression fitting technique in MATLAB (MathWorks, Natick, WA, USA). Additional details can be found in Section S12.

Salt-Sorbed Sample Preparation

Ligand-grafted samples were dialyzed for a minimum of 24 hours in periodically exchanged Milli-Q water (18.2 MΩ-cm) to remove impurities and excess starting materials. Following dialysis, the wet mass samples were equilibrated in aqueous solutions of 0.3 *m* [mol/kg] LiCl or LiOTf for a minimum of 48 hours with at least one replacement of the salt solution.

Salt Sorption Measurements

Following this equilibration, the salt-sorbed membranes were removed from solution, blotted to remove excess solution, and weighed. The salt-sorbed samples were then stirred in 80 mL of Milli-Q water (18.2 MΩ-cm) for at least 48 hours to fully desorb salt. The lithium content of the extraction solution was measured by inductively coupled plasma optical emission

spectroscopy (ICP-OES) using a Thermo Scientific Thermo iCAP 6300 ICP instrument with a sensitivity range from 10 ppb to 250 ppm.

PFG-NMR Diffusion Measurements

NMR samples were prepared by slicing salt-sorbed membranes with a razorblade into thin (~1x1x20 mm thick) slivers and sealing them in 5 mm NMR tubes with Parafilm. PFG-NMR measurements were performed on a 300 MHz (7.05 T) Bruker wide bore spectrometer equipped with a DiffBB broadband probe. Measurements were carried out at 26℃ after at least 30 minutes of equilibration, with temperature controlled by dry air at a flow rate of 800 L/hr. The self-diffusion coefficients of all nuclei were measured using a variable gradient strength stimulated echo pulse sequence. This sequence employs a stimulated echo, rather than a hard 180° pulse, in the evolution stage in order to minimize NMR signal loss while water and ions are allowed to diffuse.[17] Self-diffusion coefficients D_i, for the respective ions were determined by fitting the measured signal intensity I_i as a function of the variable gradient strength (G), using the Stejskal−Tanner equation[18, 19]

$$I = I_0 \exp\left(-D_i G^2 \gamma^2 g^2 \delta^2 \left(\Delta - \frac{\delta}{3}\right)\right) \quad (1)$$

where I_0 is the initial signal intensity, γ is the gyromagnetic ratio, δ is the gradient pulse duration, and Δ is the total diffusion time. Gradient strength values G as well as δ and Δ were carefully selected to ensure an adequate decay window to accurately determine self-diffusion. The NMR data was fitted using Topspin 4.1.4 and a MATLAB code developed in-house.

Molecular Dynamics

Atomistic molecular dynamics (MD) simulations were performed using the GROMACS MD package.[20] To maintain tractability, we chose to model the polymer as a 1:1 statistical

copolymer of PEGMEA and ligand-grafted acrylamide. Ligands are assumed to be uncharged (i.e., fully deprotonated) due to excessive Li^+ - OH^- aggregation in ligand-protonated systems. To approximate the polymer network composition of the experimental systems, the polymer network is modeled as PEGMEA appended with chains comprised of 11 polyethylene glycol (PEG) repeat units. The all-atom optimized potentials for liquid simulations (OPLS-AA),[21, 22] Madrid,[23] and TIP4P/2005[24] forcefield parametrizations were chosen to model the polymer, ions, and water respectively. The triflate anion is modeled using the OPLS-2009IL forcefield parameters.[25, 26] Simulations were performed at constant salt concentration C = 0.26 M (mol salt/L water sorbed) and water volume fraction $\phi_{\mathrm{w}} = 0.50$. Equivalent simulations on an aqueous solution (without polymer) were performed at the same salt concentration of 0.26 M. Additional details can be found in the Supporting Information.

Results and Discussion

Model Electrolyte and Polymer System

The general trade-off between water uptake and salt selectivity is a formidable obstacle for designing solute-selective membranes.[27, 28] Highly hydrated membranes tend to have high salt permeabilities and low ion-ion selectivity (i.e., low selectivity between two different solutes), while poorly hydrated membranes exhibit lower salt permeabilities but can exhibit higher ion-ion selectivity.[3, 29, 30] For this reason, the ability to independently control water uptake and ligand functionality is paramount for elucidating their respective roles in facilitating solute-selective transport within ligand functionalized membranes. While macroscopic permeation and conductivity measurements have been widely applied to characterize transport in both charged and uncharged PEGDA networks, to date only a small number of functionalized networks have been explored.[1, 8, 31-37] Historically, the design of new functional networks has been hindered by

reactivity ratio differences and monomer compatibility requiring careful synthetic optimization for each new system. The polyethylene glycol diacrylate (PEGDA) based co-polymer network enables a broad range of functionalized membranes to be synthesized while offering simultaneous control of cross-linking density and membrane hydration. The network chemistry chosen here is shown in **Figure 1** and composed of four monomer building blocks: polyethylene glycol diacrylate (PEGDA) as crosslinker, hydrophilic PEG methyl ether acrylate (PEGMEA) and hydrophobic butyl acrylate (BA) to tune water uptake, and pentafluorophenyl acrylate (PFPA) as active ester monomer that can be readily functionalized with various amine-containing ligands to modulate salt solubilization and ligand-ion interactions. As all four acrylate monomers have relatively similar reactivity ratios (e.g., 1.4 and 0.22 for PFPA and PEG acrylate, respectively)[38] we assume effectively random incorporation of PFPA and other monomer groups throughout the polymer networks.

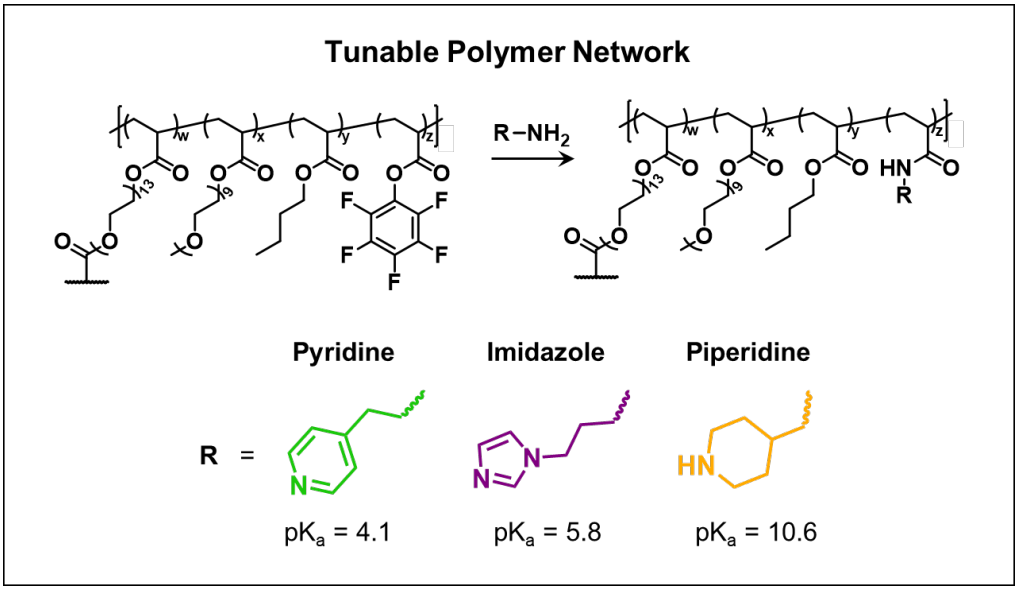

Figure 1. Schematic of the post-polymerization functionalization of the parent random co-polymer network (top) to give a library of derivatives comprised of $(PEGDA)_w$, $(PEGMEA)_x$, $(BA)_y$ and $(acrylamide)_z$, with "**R"** representing one of three nitrogen heterocycle ligands (bottom).

The determination of water, cation, and anion self-diffusion coefficients is critical to establish a complete understanding of solute-selective membrane separation processes. Unfortunately, PFG-NMR measurements are not practical for many traditionally investigated ions (e.g. Na^+, Cl^-, NO_3^-, SO_4^{2-}) due to rapid NMR signal loss over the course of the measurement, and/or to the inherently low NMR sensitivity of the constituent nuclei.[39] To overcome these limitations, we investigate a model electrolyte (cf. **Figure 2**) consisting of a water-soluble LiOTf salt enabling self-diffusion measurements of water molecules, the Li^+ cation, and the OTf^- anion using ^1H, ^7Li and ^{19}F PFG-NMR (respectively).[40] It is worth noting that PFG-NMR measurements attempted on an analogous NaOTf electrolyte proved unsuccessful due to short ^{23}Na T_2 relaxation times, resulting in complete (^{23}Na) signal attenuation during the application of the spatially encoding gradient pulse and convoluting the interpretation of the results.

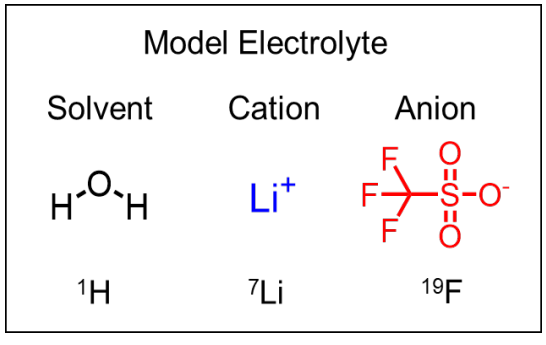

Figure 2. Model electrolyte system with NMR active nuclei labeled for the solvent (^{1}H), cation (^{7}Li), and anion (^{19}F), respectively.

Role of Ligand pK$_a$ on Membrane Swelling and Transport

The role of ligand polarity (quantified by the effective pK$_a$) on ion-ligand interactions is a central question surrounding the design of solute-selective membranes. To address this question, we first investigate the effects of ligand Lewis basicity on water uptake and transport using 28 / 20 / 52 mol% PEGDA / PEGMEA / acrylamide random co-polymer networks grafted with one of three different ligands with membrane pK$_a$ values ranging from 4.1 to 10.6. Ligand grafting densities were chosen to be in the approximate range of commercial ion exchange membranes (i.e., ~1.2-2 mmol/g dry polymer)[41], where the charge density of the membranes is dictated by the extent of protonation of the tethered ligand, as depicted in **Figure 3**. Less basic ligands such as pyridine (membrane pK$_a$ = 4.1) exhibit very weak protonation when the membranes are sorbed (swollen) with neutral pH water, resulting in a very low effective fixed charge concentration (cf., **Table 1**). More basic ligands such as piperidine (membrane pK$_a$ = 10.6) yield much higher effective fixed charge densities as the equilibrium shifts to predominantly favor the protonated species at near neutral pH. Effective fixed charge densities are estimated from the Hendersen-Hasselbach equation by measuring both the pK$_a$ of the membranes, as described above, and the pH of salt solutions in equilibrium with the membranes following salt sorption:

$$pH = pK_a + \log\frac{[L]}{[HL^+]} \tag{2}$$

$$\alpha_{H^+} = \frac{[HL^+]}{[HL^+]+[L]} = \frac{1}{1+\log^{-1}(pH-pK_a)} \tag{3}$$

where $[L]$ and $[HL^+]$ are the concentrations of deprotonated and protonated ligands, respectively, and α_{H^+} is the fraction of protonated ligands in the system.[42, 43] Total ligand concentration values (i.e., $[HL^+] + [L]$) are known from the co-monomer ratios of the respective polymer networks.

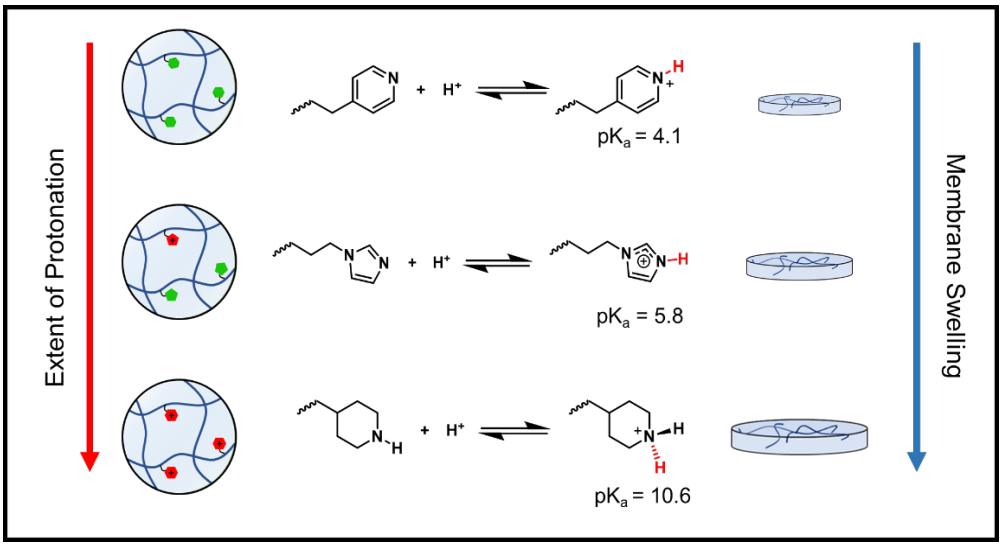

Figure 3. Depiction of ligand protonation equilibrium reactions for the three ligands investigated in this work, demonstrating the increased extent of protonation and membrane swelling with increasing ligand pK_a.

Consistent with previous findings, water uptake measurements (presented as water volume fractions, ϕ_w, in **Figure 4**) demonstrate that ligand polarity directly impacts membrane hydrophobicity.[6] Membrane hydration is shown to increase with increasing ligand basicity (i.e., increasing pK_a) due to increased protonation of the ligand pendant groups, which in turn enhances the hydrophilicity of the polymer network and further induces swelling due to electrostatic repulsions between the polymer chains.[44, 45] Thus, membrane water uptake can be directly tuned by altering the number of repulsive electrostatic interactions between protonated ligands by controlling both the basicity of the covalently bonded ligands, as well as the ligand grafting density independently.

Table 1. Ligand pK_a values, ligand densities, pH values, protonation fractions and effective fixed charge concentrations of 28 / 20 / 52 mol% PEGDA / PEGMEA / acrylamide membranes with different amines equilibrated in 0.3 *m* [mol/kg] LiOTf.

Ligand	Membrane pK_a	mmol Ligand/g Dry Polymer	mmol Ligand/cm^3 Swollen	pH	Fraction Protonated Ligands	mmol Charge/cm^3 Swollen
Pyridine	4.1	1.37	0.757	5.54	0.035	0.027
Imidazole	5.8	1.37	0.710	6.54	0.15	0.11
Piperidine	10.6	1.39	0.482	6.40	1.00	0.48

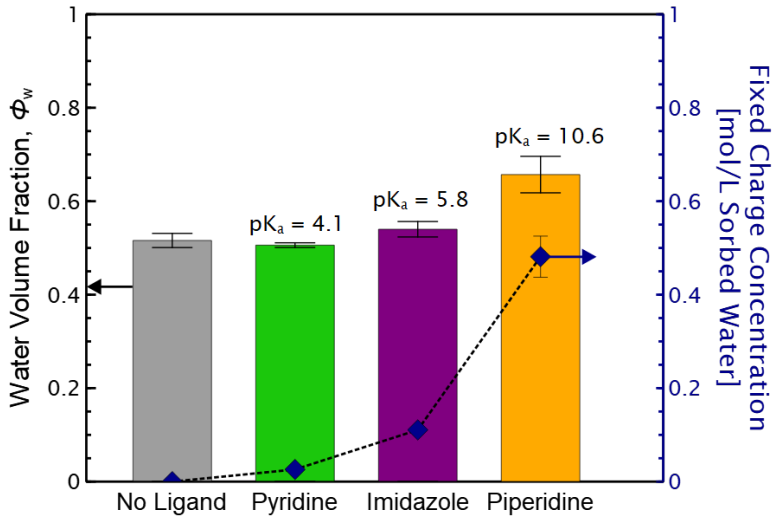

Figure 4. Water volume fraction ϕ_w (left axis) and fixed charge concentrations indicated by blue diamonds (right axis) for 28 / 20 / 52 mol% PEGDA / PEGMEA / acrylamide membranes substituted with different amines equilibrated in a 0.3 M LiOTf electrolyte solution. Ligand-free control networks are 41 / 59 mol% PEGDA / PEGMEA.

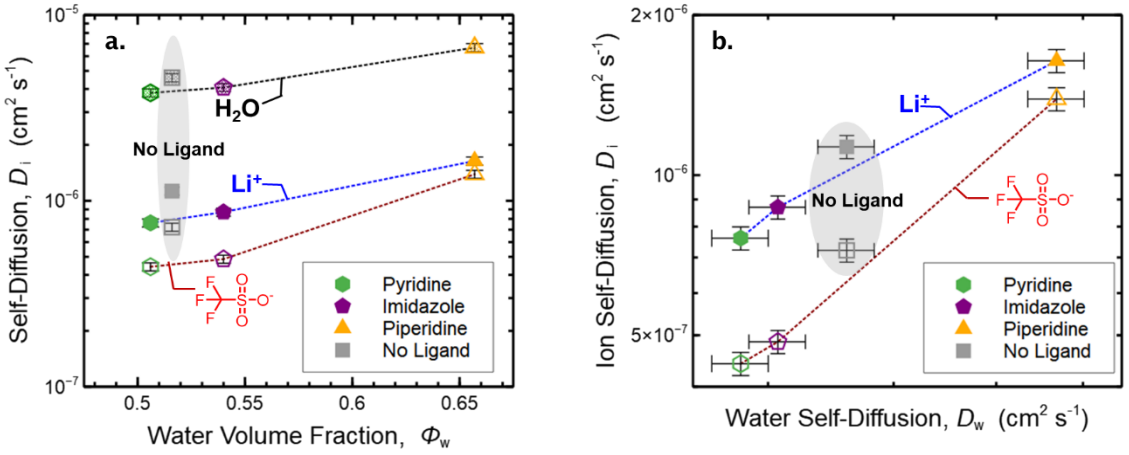

Figure 5. Self-diffusion coefficients of Li^+ (filled markers) and OTf^- (unfilled markers) ions plotted vs. (a) water volume fraction ϕ_w, and (b) water self-diffusion coefficients D_w, for 28 / 20 / 52 mol% PEGDA / PEGMEA / acrylamide membranes substituted with different amines equilibrated in a 0.3 *m* [mol/kg] LiOTf electrolyte solution. Ligand-free control networks are 41 / 59 mol% PEGDA / PEGMEA. Water self-diffusion coefficients are also shown in (a) as lightly shaded markers.

PFG-NMR self-diffusion measurements reveal that the water volume fraction (i.e., membrane hydration) plays a role in ion and water transport within the membrane (cf. **Figure 5a**), with the self-diffusion of both ions strongly coupled to the self-diffusion of water (cf. **Figure 5b**). However, the influence of ligand chemistry on ligand-ion interactions is less clear. Ion and water self-diffusion coefficients are notably faster in the non-functionalized (no ligand) membranes compared to imidazole and pyridine membranes of similar water content, suggesting that ion-ligand interactions may act to impede ion transport, as previously observed in molecular dynamics simulations.[46, 47] These findings are consistent with the observations of Moon et al.[6]

Impact of Membrane Hydration on Water and Ion Transport

Table 2. Compositions of PEGDA polymer networks with varying butyl acrylate (BA) co-monomer fractions. Note the decrease in dry ligand density (mmol ligand/g dry polymer) in the networks containing 2.9 moles of BA due to the replacement of acrylamide with butyl acrylate in order to achieve the desired hydrophobicity.

Moles BA	Membrane Type	PEGDA (mol%)	BA (mol%)	PEGMEA (mol%)	Acrylamide (mol%)	mmol ligand /g dry polymer
0	No Ligand	41	0	59	0	0
	Ligand	28	0	20	52	1.36
1.7	No Ligand	26	55	19	0	0
	Ligand	20	43	0	37	1.44
2.9	No Ligand	21	75	4	0	0
	Ligand	19	69	0	12	0.49

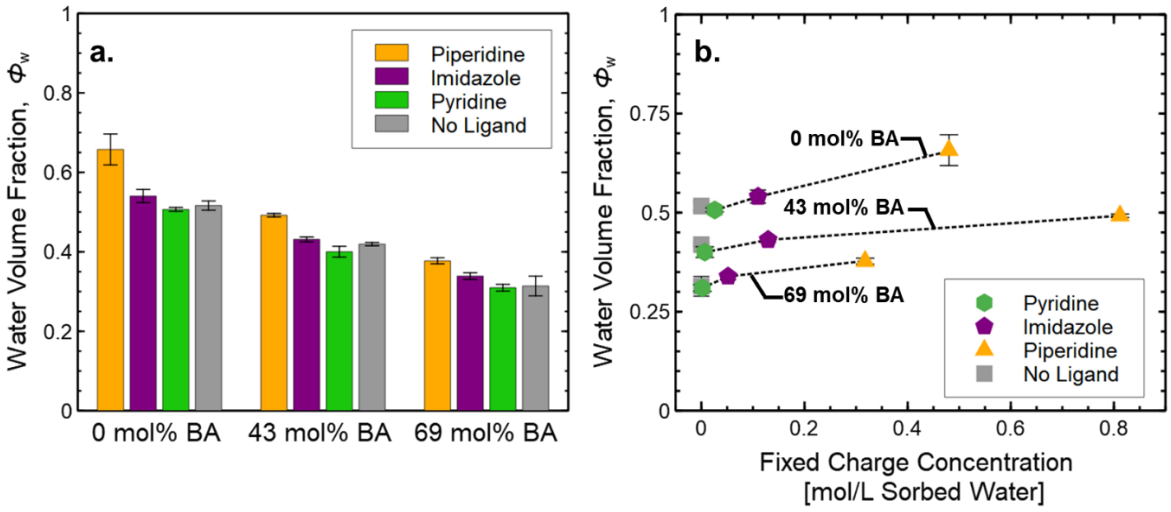

Figure 6. (a) Water volume fraction, ϕ_w, vs. mol% of butyl acrylate (BA) co-monomer for hydrogel compositions outlined in **Table 2**. (b) Water volume fraction, ϕ_w, vs. fixed charge concentration (i.e., concentration of protonated ligands) for pyridine (green octagons), imidazole (purple pentagons), piperidine (yellow triangles) ligands, and a ligand-free control network

(grey squares), equilibrated in 0.3 *m* [mol/kg] LiOTf electrolyte solutions. Lines in (b) are provided as a visual guide.

In order to decouple the effects of membrane hydration and ligand chemistry on water and ion transport, we modulate the membrane water uptake by replacing some of the hydrophilic PEGMEA monomer with the hydrophobic BA monomer in the compositions outlined in **Table 2**. The water volume fractions of polymers containing different molar fractions of BA monomer, plotted in **Figure 6a**, demonstrate that membrane hydration can be systematically reduced through the increasing incorporation of hydrophobic BA repeat units in the parent network structure. Notably, the extent of ligand protonation (i.e., fixed charge concentration) continues to influence membrane hydration even at the highest BA compositions (cf. **Figure 6b**). It should be noted that the 43 mol% BA piperidine and imidazole grafted membranes have larger effective fixed charge concentrations than their respective 0 mol% BA analogues as the 0 mol% BA and 43 mol% BA membranes have similar dry ligand grafting densities, but the 43 mol% BA membranes have lower water uptake and thus smaller total volumes. Leveraging this synthetic control mechanism over membrane hydration, we investigate the relative influence of ligand chemistry on transport properties as a function of membrane water content.

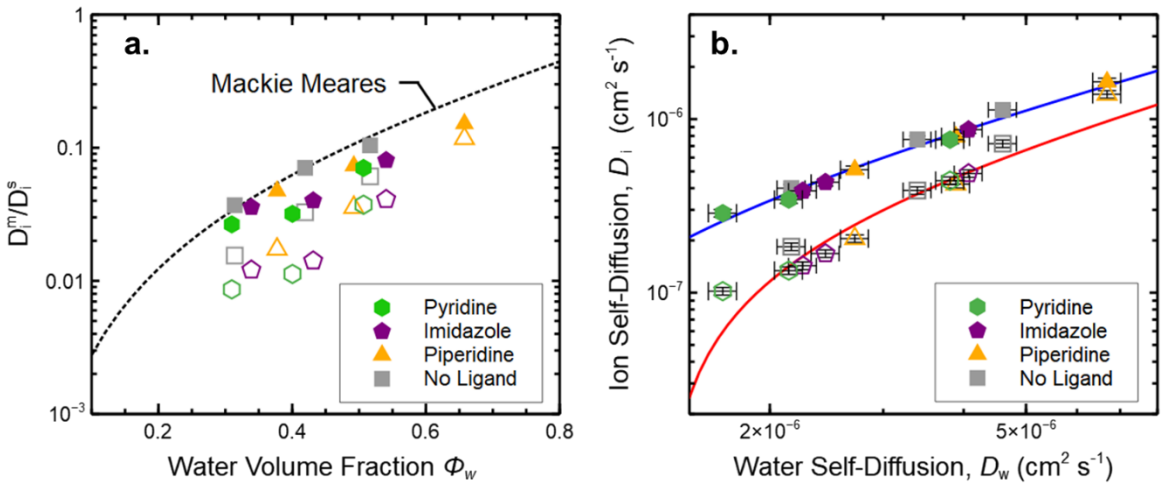

Figure 7. (a) Self-diffusion coefficients for Li^+ (filled markers) and OTf^- (unfilled markers) ions in the membranes of interest to this work (D_i^m), normalized over their self-diffusion coefficient in an aqueous solution (D_i^s) and plotted as a function of water volume fraction, ϕ_w. The dashed black line represents the prediction from the Mackie and Meares model. (b) Li^+ (filled markers) and OTf^- (unfilled markers) diffusion coefficients (D_i) plotted as a function of the water self-diffusion coefficients (D_w) in the membranes. The solid lines represent linear regressions ($D_i = D_w m + D_0$) included to guide the eye. The results shown here were obtained on hydrogels containing pyridine (green octagons), imidazole (purple pentagons), and piperidine (yellow triangles) ligands, and a ligand-free control network (grey squares), equilibrated in 0.3 m [mol/kg] LiOTf electrolyte solutions.

Consistent with the results shown above, PFG-NMR measurements reveal that water and ion self-diffusion coefficients are directly correlated to the water volume fraction of the membrane. This suggests that membrane tortuosity and network structure play significant roles in ion and water transport. To probe membrane tortuosity effects, we compare self-diffusion coefficients measured by PFG-NMR to self-diffusion values predicted using the widely-applied Mackie and

Meares model.[48] This obstruction-based model approximates the membrane as a cubic lattice comprised of interwoven water and impermeable fixed polymer domains[22], in which solute diffusion is restricted to the water domains of the membrane. Within these water domains, the self-diffusion of a given solute (D_i^m) is assumed to be equivalent to its self-diffusion in aqueous solution (D_i^s). Under this assumption, the Mackie and Meares model exclusively accounts for tortuosity effects, where immobile polymer chains impede transport by acting as physical barriers that ions and water molecules must diffuse around. Thus, the self-diffusion of a given species within the membrane D_i^m can be predicted from its aqueous solution self-diffusion coefficient D_i^s and the polymer water volume fraction ϕ_w.

$$\frac{D_i^m}{D_i^s} = \left(\frac{\phi_w}{2-\phi_w}\right)^2 \quad (4)$$

As observed in **Figure 7**, for membranes with the same ligand functionalization and different degrees of hydration (i.e., different BA compositions), the cation and anion follow the general trend of decreasing diffusivity with decreasing water volume fraction, which is qualitatively consistent with the Mackie and Meares model. This suggests that tortuosity plays a role in controlling ion diffusion when the membrane chemistry and network density is constant. However, the Mackie and Meares model overpredicts the self-diffusion coefficients of Li^+ and OTf^- in most of the ligand functionalized membranes, particularly for the OTf^- anion. Notably, the model demonstrates better predictability of Li^+ transport within the ligand-free hydrogel, with predicted values in good agreement with experimental Li^+ self-diffusion values, but it still systematically overpredicts OTf^- self-diffusion coefficients for this system. Due to the lack of molecular detail in the Mackie and Meares model, it is difficult to pinpoint the exact source of the observed deviations; however, the large disagreements suggest that ion-polymer interactions are

partly responsible for impeding ion transport within the ligand-functionalized membranes. The deviation $R_{D,i} = (D^m_{i,MM} - D^m_{i,Exp})/D^s_i$ between the experimentally measured self-diffusion coefficient ($D^m_{i,Exp}$) and that predicted by the Mackie and Meares model ($D^m_{i,MM}$), normalized by the self-diffusion coefficient in solution (D^s_i), is plotted for Li^+ and OTf^- in **Figure S6**. $R_{D,i}$ increases with membrane water content, suggesting that membrane hydration is primarily responsible for the deviation of the experimentally measured self-diffusion values from the value predicted using the obstruction-based Mackie and Meares model, with ligand chemistry playing a secondary role.[46] Interestingly, the Li^+/ OTf^- diffusion-selectivity ratios $(\frac{D_{Li^+}}{D_{OTf^-}})$ presented in **Figure 8** demonstrate enhanced Li^+ selective transport with decreasing water volume fraction, irrespective of whether the membrane water content is controlled by the BA monomer fraction or by the chemistry of the tethered ligand.

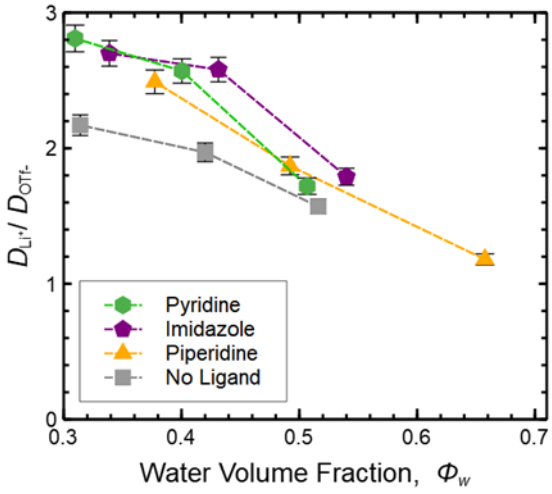

Figure 8. Self-diffusion selectivity of Li^+ over OTf^- $\left(\frac{D_{Li^+}}{D_{OTf^-}}\right)$ vs. water volume fraction, ϕ_w, for hydrogels containing pyridine (green octagons), imidazole (purple pentagons), and piperidine

(yellow triangles) ligands, and a ligand-free control network (grey squares) equilibrated in 0.3 *m* [mol/kg] LiOTf electrolyte solutions. Lines are provided as a visual guide.

Comparison between LiOTf and LiCl electrolytes

Given the ubiquity of chloride (Cl^-) anions in water treatment and mineral recovery systems, Cl^- is a relevant solute for practical membrane separations. Here, we compare the transport properties of our model LiOTf electrolyte to a 0.3 *m* [mol/kg] LiCl electrolyte for all hydrogels of interest to this work. We first compare the salt sorption coefficient of LiOTf and LiCl, K_s, defined as the ratio of the salt concentration within the total volume of the swollen membrane (i.e. polymer, water, and salt), $C_{salt}^{m,p}$, to the concentration of the external solution, C_{salt}^{s}, and which quantifies the propensity of the salt to integrate the water swollen membrane.

$$K_s = \frac{C_{salt}^{m,p}}{C_{salt}^{s}} \quad (6)$$

ICP measurements reveal significantly greater sorption of LiOTf compared to LiCl by all membrane compositions. In **Figure 9** we compare the salt sorption coefficients in terms of the model proposed by Yasuda et al.[49]

$$K_s = \phi_p K_p + \phi_w K_w \quad (7)$$

where ϕ_p and ϕ_w are the volume fractions of polymer and water, respectively, and K_p and K_w the sorption coefficients within the polymer and water domains of the membrane. In the limiting case where no salt is present in the polymer network (K_p = 0) and the concentration of salt present in the water domains of the membrane is equal to that of the contiguous aqueous electrolyte ($K_w = 1$), the total membrane salt sorption coefficient is equal to the water volume fraction of the membrane (i.e., $K_s = \phi_w$). K_s values obtained for the LiCl and LiOTf electrolytes reveal significant membrane selectivity for the OTf^- anion, indicating that ion-polymer interactions

and/or partial ion dehydration (i.e., fewer water molecules in the anion hydration shell) are more prevalent in LiOTf-containing membranes.[50] These hypotheses are supported by the MD simulation results discussed in the next section.

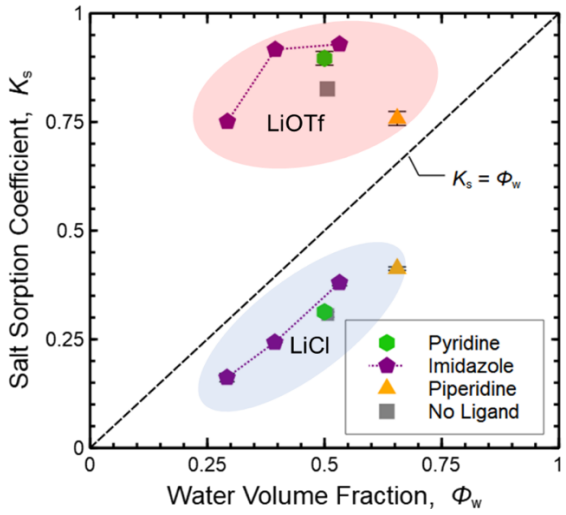

Figure 9. Relationship between salt sorption coefficient, K_s, and water volume fraction, ϕ_w, for hydrogels containing pyridine (green octagons), imidazole (purple pentagons), and piperidine (yellow triangles) ligands, and a ligand-free control network (grey squares) equilibrated in 0.3 *m* LiCl and LiOTf electrolyte solutions. Purple dashed lines are provided as a visual guide. The black dashed line at $K_s = \phi_w$ represents the limiting case where no salt is present in the polymer network ($K_p = 0$) and the concentration of salt present in the water domains of the membrane is equal to that of the contiguous aqueous electrolyte ($K_w = 1$).

The salt sorption values presented in **Figure 9** for LiCl and LiOTf fall on opposite sides of the limiting case (i.e., $K_s = \phi_w$). As both electrolytes share a common Li^+ cation, the difference in solute sorption selectivity can be attributed to anion-polymer interactions. For the LiCl-sorbed systems, $K_s < \phi_w$ and the membranes demonstrate solute selectivity for water over LiCl salt, (i.e.,

the membranes preferentially sorb water over the LiCl salt). On the other hand, for the LiOTf-sorbed systems, $K_s > \phi_w$ and the membranes demonstrate solute selectivity for LiOTf salt over water. Hence, some fraction of LiOTf salt resides in polymer-rich domains within the membrane ($K_p > 0$) since anion-polymer interactions are stronger than water-polymer interactions[31]. The high sorption of LiOTf has been observed for other organic ions and is attributed to the lower hydration energy of relatively large organic anions.[5, 51-54] In this case, OTf^- anions more readily dehydrate allowing them to directly interact with the polymer, thereby decreasing the free energy difference between the aqueous electrolyte and the membrane.[33, 55] This explains the increased selectivity of the membrane to the larger OTf^- anion compared to the smaller Cl^- anion.[46] In turn, this enhanced anion selectivity draws more Li^+ ions into the membrane to maintain charge neutrality, resulting in a greater overall salt concentration within the membrane. This is corroborated by our relative hydration calculations from molecular dynamics simulations discussed in the following section. Further analysis of the salt sorption measurements found in the supporting information (**Figure S2**) reveals no clear dependence on the (membrane) fixed charge concentration suggesting that Donnan exclusion effects have a minimal influence on salt partitioning. This is attributed to the weakly charged nature of the membranes ($0 < C_{swoll}^{LH+} < 0.5$ mol/L) compared to salt concentration of the external electrolyte (~0.3 mol/L) and is consistent with previous investigations and theory surrounding weakly charged membranes.[7-9, 56]

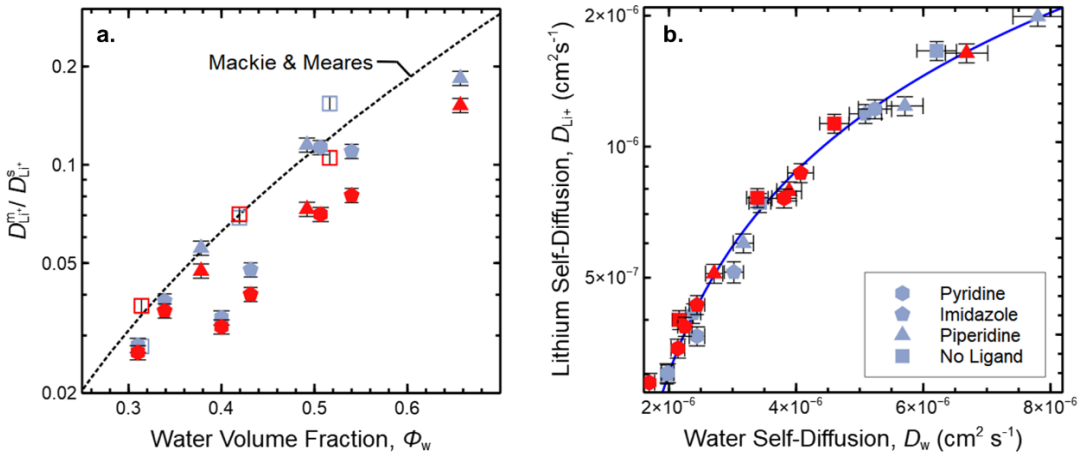

Figure 10. Overview of the influence of water uptake and dynamics on Li^+ transport properties for the complete set of systems investigated in this work**.** (a) Li^+ self-diffusion coefficient in the membrane ($D^m_{Li^+}$) normalized by the Li^+ self-diffusion coefficient in solution ($D^s_{Li^+}$) and plotted as a function of the water volume fraction, ϕ_w, with the dashed black line representing Mackie and Meares predictions. (b) Li^+ self-diffusion coefficient plotted as a function of the water self-diffusion coefficient, with the solid blue line providing a visual guide. Results obtained on hydrogels containing pyridine (octagons), imidazole (pentagons), and piperidine (triangles) ligands, and a ligand-free control network (squares) equilibrated in 0.3 *m* [mol/kg] LiCl (blue symbols) and LiOTf (red symbols) electrolyte solutions.

The self-diffusion coefficients presented in **Figure 10** demonstrate greater water and Li^+ mobility in membranes sorbed with LiCl electrolyte compared to LiOTf electrolytes. In contrast to the LiOTf-sorbed membranes, the Mackie and Meares model (cf. **Figure 10a**) is generally consistent with experimental self-diffusion coefficients obtained for the Li^+ cation in LiCl sorbed membranes, indicating that Li^+-polymer interactions play a minimal role in the transport properties of LiCl-sorbed membranes. Overall, the results presented in this section highlight the critical role of anion hydration energy in salt selectivity and the transport properties of the membranes.

Specifically, the lower hydration energy of the OTf^- anion leads to enhanced salt sorption (i.e., greater membrane salt concentrations) and increased anion-polymer interactions, both of which act to impede the transport of all diffusing species (i.e., lithium, triflate, and water) within the membrane.

Molecular Dynamics Simulation Results

We turn to atomistic molecular dynamics (MD) simulations to obtain molecular-level insights into the interactions underpinning the transport properties of the hydrogel systems of interest. The simulations were performed on the different ligand-functionalized polymer networks of interest to this work at a constant salt concentration of C = 0.26 M relative to the volume of sorbed water and at a fixed water volume fraction of $\phi_w = 0.50$, as well as on aqueous solutions of similar salt concentration, as described in more detail in the experimental section. The simulation results corroborate our experimental observations that ion solvation plays a more significant role than ion-ligand interactions in ion and water transport in those membranes.

First, we find that Li^+ diffusivities computed for the different ligand-functionalized polymer networks do not vary significantly with ligand chemistry (see **Figure S8**), suggesting that Li^+-ligand interactions do not play a substantial role in governing Li^+ ion transport in these systems. We note that the diffusion coefficients obtained from the simulations are not directly comparable to those obtained from PFG-NMR, as a simpler polymer model was used in the molecular dynamics runs (see experimental section). However, trends across the various membrane and aqueous solution systems are meaningful. Secondly, radial distribution functions and coordination functions for Li^+, OTf^-, and Cl^- salt ions derived for each of the membranes of interest and for aqueous solutions, as explained in **Section S11.5**, are shown in **Figures S9-S13**. For the membrane systems, the ion-water coordination numbers presented in **Figures S9** and **S10** do not vary

significantly with ligand chemistry. Hence, the hydration and diffusive slowdown of ions upon transfer from solution to membrane are averaged across all of the ligand-functionalized polymer networks for the LiOTf and LiCl salts, respectively, in **Figure 11**. The relative hydration of Li^+ and OTf^- ions, shown in **Figure 11a**, is defined as the ratio of the average ion-water coordination number in the salt-sorbed membrane ($n_{H_2O}^m$) to that in the aqueous solution ($n_{H_2O}^s$), where the ion-water coordination number is the value of the coordination distribution function at the first minimum in the radial distribution function in **Figure S9**. The relative hydration of the ion represents the fraction of water molecules in its first hydration shell that is maintained when the ion moves from the aqueous solution to the hydrated membrane. This ratio is close to 1 for Li^+ and explains why Li^+ transport is highly correlated to water content and water dynamics within the membrane. Consistent with this result, the radial distribution and coordination functions for PEO and ligand functionalities around the Li^+ ion, shown in **Figure S11**, indicate a much lower coordination to the polymer than to water (**Figure S9a**). Hence, increasing membrane water content increases the available "wet" pathways for Li^+ ion and water transport to occur, thus increasing their dynamics. Interestingly, OTf^- appears to dehydrate substantially reducing its hydration number from ~10 waters to ~4-5 waters upon transfer from solution to membrane (**Figure S9b**). By retaining only part of its hydration shell in the membrane, OTf^- preferentially resides in polymer-rich regions in close proximity to the PEO and ligand functionalities. This is demonstrated by the magnitude of the first correlation peak (greater than unity) in the radial distribution functions for PEO and ligand functionalities around the OTf^- anion obtained from the simulations, as shown in **Figure S12a**, indicating a greater than average density of polymer around OTf^-. The strong interactions between OTf^- and the polymer may also explain why OTf^- experiences a greater diffusive slowdown (smaller D_i^m/D_i^s) upon transfer from solution to

membrane compared to Li^+ (**Figure 14b**), and consequently why it diffuses more slowly than Li^+ in the membrane despite having a higher self-diffusion coefficient than Li^+ in solution (**Figure S8**). We note that the average Li^+ diffusive slowdowns (D_i^m/D_i^s) computed for the LiOTf and LiCl membrane systems, of 0.052 and 0.069, respectively (see **Figure 11b**), agree well with the average values obtained from the ^{7}Li PFG-NMR experiments at a water volume fraction $\phi_w = 0.5$, of about 0.075 and 0.11 for LiOTF and LiCl (see **Figure 10a**). The tendency for Li^+ ions to retain their coordination with water in the presence of ligands in an aqueous environment has been observed previously and has been attributed to lithium's relatively large hydration free energy compared to other monovalent ions.[3] Further, the relative hydration of cations has been shown to follow the trend in hydration free energy, that is, cations with a lower hydration free energy shed more waters upon transfer from solution to the membrane.[46] Similarly, we expect the tendency of OTf^- anions to shed their hydrating water to arise from a low hydration free energy due to the lower charge density of the bulky anion, therefore, triflate anions more favorably interact with the lower mobility (fewer degrees of freedom than water) and lower dielectric polymer.[51] This is apparent when comparing OTf^- to Cl^-, whereby Cl^-, similarly to Li^+, retains its hydration shell (**Figure 11a**) due to its high charge density and hydration free energy. Unlike OTf^-, Cl^- is repelled by the polymer, as indicated by the radial distribution functions shown in **Figure S12b**, and experiences a smaller diffusive slowdown (**Figure 11b**) and maintains a higher self-diffusion coefficient than Li^+ in both membrane and aqueous solution systems (**Figure S8**).

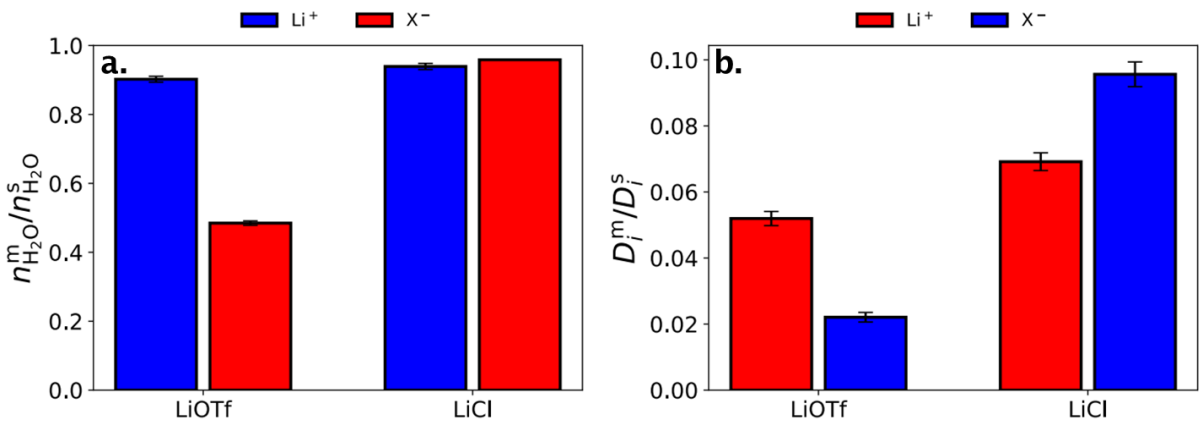

Figure 11. (a) Relative hydration of Li^+ and X^- (OTf^-, Cl^-), where relative hydration is defined as the ratio of the average ion-water coordination number in the salt-sorbed membrane ($n^m_{H_2O}$), to that in an aqueous solution ($n^s_{H_2O}$) at similar salt concentrations. (b) Ratio of the Li^+ and X^- (OTf^-, Cl^-) self-diffusion coefficients in the membrane (D^m_i) and in an aqueous solution (D^s_i). The coordination numbers and self-diffusion coefficients are obtained from separate molecular dynamics simulations on each of the membrane and aqueous solution systems of interest to this work, and the results displayed here are averaged over all membrane systems (No Ligand, Pyridine, Imidazole, Piperidine).

Conclusions

This work provides insight into the influence of membrane chemistry and hydration on microscopic-scale ion and water diffusion in weakly-charged polymer membranes. By coupling synthesis of well-controlled ligand-functionalized membranes using active ester chemistry with direct measurements of water and ion self-diffusion coefficients using PFG-NMR, for membranes sorbed with an NMR-active LiOTf electrolyte, it is found that membrane water content is the predominant driver of ion self-diffusion. Further, ion self-diffusion is coupled to the self-diffusion of water. Despite the dominant role of membrane hydration, experimental self-diffusion

coefficients deviate from predicted values using the Mackie and Meares model, suggesting that anion-ligand and ion-polymer interactions slow transport in addition to tortuosity effects. The importance of such interactions is consistent with results from salt sorption measurements, showing enhanced LiOTf sorption compared to LiCl, indicating favorable OTf^- polymer interactions. Molecular dynamics simulations further reveal partial dehydration of OTf^- anions in the presence of polymer chains leading to direct-ion polymer interactions. These findings offer important insights into the rational design of solute-selective membranes, while highlighting the importance of anion identity on membrane-solute interactions and providing pathways for future synthetic developments.

Supporting Information

Experimental details for the Pentafluorophenyl acrylate monomer synthesis, membrane fabrication, characterization techniques and data, as well as simulation details and forcefield parameters can be found in the Supporting Information.

Acknowledgements

This work was primarily supported as part of the Center for Materials for Water and Energy Systems (M-WET), an Energy Frontier Research Center funded by the U.S. Department of Energy, Office of Science, Basic Energy Sciences under Award #DE-SC0019272. The NMR and ICP-OES measurements made use of shared facilities of the National Science Foundation (NSF)-supported Materials Research Science and Engineering Center (MRSEC) at UC Santa Barbara, NSF DMR-1720256. The UCSB MRSEC is a member of the Materials Research Facilities Networks (www.mrfn.org). The MD simulation results in this paper were generated using high-

performance computing resources provided by The University of Texas at Austin Texas Advanced Computing Center.

References

(1) Landsman, M. R.; Sujanani, R.; Brodfuehrer, S. H.; Cooper, C. M.; Darr, A. G.; Davis, R. J.; Kim, K.; Kum, S.; Nalley, L. K.; Nomaan, S. M.; et al. Water Treatment: Are Membranes the Panacea? *Annu Rev Chem Biomol Eng* 2020, *11*, 559-585. DOI: 10.1146/annurev-chembioeng-111919-091940

(2) Jegatheesan, V.; Shu, L.; Jegatheesan, L. Producing fit-for-purpose water and recovering resources from various sources: An overview. *Environmental Quality Management* 2021, *31* (2), 9-28. DOI: 10.1002/tqem.21780

(3) Warnock, S. J.; Sujanani, R.; Zofchak, E. S.; Zhao, S.; Dilenschneider, T. J.; Hanson, K. G.; Mukherjee, S.; Ganesan, V.; Freeman, B. D.; Abu-Omar, M. M.; et al. Engineering Li/Na selectivity in 12-Crown-4-functionalized polymer membranes. *Proc Natl Acad Sci U S A* 2021, *118* (37). DOI: 10.1073/pnas.2022197118

(4) Sujanani, R.; Landsman, M. R.; Jiao, S.; Moon, J. D.; Shell, M. S.; Lawler, D. F.; Katz, L. E.; Freeman, B. D. Designing Solute-Tailored Selectivity in Membranes: Perspectives for Water Reuse and Resource Recovery. *ACS Macro Lett* 2020, *9* (11), 1709-1717. DOI: 10.1021/acsmacrolett.0c00710

(5) Epsztein, R.; Shaulsky, E.; Qin, M.; Elimelech, M. Activation behavior for ion permeation in ion-exchange membranes: Role of ion dehydration in selective transport. *Journal of Membrane Science* 2019, *580*, 316-326. DOI: 10.1016/j.memsci.2019.02.009

(6) Moon, J. D.; Sujanani, R.; Geng, Z. S.; Freeman, B. D.; Segalman, R. A.; Hawker, C. J. Versatile Synthetic Platform for Polymer Membrane Libraries Using Functional Networks. *Macromolecules* 2021, *54* (2), 866-873. DOI: 10.1021/acs.macromol.0c02414

(7) Kitto, D.; Kamcev, J. Manning condensation in ion exchange membranes: A review on ion partitioning and diffusion models. *Journal of Polymer Science* 2022, *60* (21), 2929-2973. DOI: 10.1002/pol.20210810

(8) Yan, N.; Sujanani, R.; Kamcev, J.; Galizia, M.; Jang, E. S.; Paul, D. R.; Freeman, B. D. Influence of fixed charge concentration and water uptake on ion sorption in AMPS/PEGDA membranes. *Journal of Membrane Science* 2022, *644*. DOI: 10.1016/j.memsci.2021.120171

(9) Yan, N.; Sujanani, R.; Kamcev, J.; Jang, E. S.; Kobayashi, K.; Paul, D. R.; Freeman, B. D. Salt and ion transport in a series of crosslinked AMPS/PEGDA hydrogel membranes. *Journal of Membrane Science* 2022, *653*. DOI: 10.1016/j.memsci.2022.120549

(10) Kamcev, J.; Paul, D. R.; Freeman, B. D. Ion Activity Coefficients in Ion Exchange Polymers: Applicability of Manning's Counterion Condensation Theory. *Macromolecules* 2015, *48* (21), 8011-8024. DOI: 10.1021/acs.macromol.5b01654

(11) Kamcev, J.; Paul, D. R.; Manning, G. S.; Freeman, B. D. Predicting Salt Permeability Coefficients in Highly Swollen, Highly Charged Ion Exchange Membranes. *ACS Appl Mater Interfaces* 2017, *9* (4), 4044-4056. DOI: 10.1021/acsami.6b14902

(12) Yu, Y.; Yan, N.; Freeman, B. D.; Chen, C. C. Mobile ion partitioning in ion exchange membranes immersed in saline solutions. *Journal of Membrane Science* 2021, *620*. DOI: 10.1016/j.memsci.2020.118760

(13) Garrido, L.; Pozuelo, J.; Lopez-Gonzalez, M.; Yan, G.; Fang, J.; Riande, E. Influence of the water content on the diffusion coefficients of Li+ and water across naphthalenic based copolyimide cation-exchange membranes. *J Phys Chem B* 2012, *116* (38), 11754-11766. DOI: 10.1021/jp3065322

(14) Abbaszadeh, M.; Garell, M.; Il Choi, J.; Chen, Y. D.; Leisen, J.; Jang, S. S.; Hu, Y. Y.; Hatzell, M. C. Unraveling Water and Salt Transport in Polyamide with Nuclear Magnetic Resonance Spectroscopy. *Acs Materials Letters* 2022, *5* (2), 291-298. DOI: 10.1021/acsmaterialslett.2c00932

(15) Kalakkunnath, S.; Kalika, D. S.; Lin, H. Q.; Freeman, B. D. Viscoelastic characteristics of UV polymerized poly(ethylene glycol) diacrylate networks with varying extents of crosslinking. *Journal of Polymer Science Part B-Polymer Physics* 2006, *44* (15), 2058-2070. DOI: 10.1002/polb.20873

(16) Lin, H. Q.; Kai, T.; Freeman, B. D.; Kalakkunnath, S.; Kalika, D. S. The effect of cross-linking on gas permeability in cross-linked poly(ethylene glycol diacrylate). *Macromolecules* 2005, *38* (20), 8381-8393. DOI: 10.1021/ma0510136

(17) Tanner, J. E. Use of the Stimulated Echo in NMR Diffusion Studies. *The Journal of Chemical Physics* 1970, *52* (5), 2523-2526. DOI: 10.1063/1.1673336

(18) Stejskal, E. O.; Tanner, J. E. Spin Diffusion Measurements: Spin Echoes in the Presence of a Time-Dependent Field Gradient. *Journal of Chemical Physics* 1965, *42* (1). DOI: 10.1063/1.1695690

(19) Sinnaeve, D. The Stejskal-Tanner equation generalized for any gradient shape-an overview of most pulse sequences measuring free diffusion. *Concepts in Magnetic Resonance Part A* 2012, *40a* (2), 39-65. DOI: 10.1002/cmr.a.21223

(20) Abraham, M. J.; Murtola, T.; Schulz, R.; Páll, S.; Smith, J. C.; Hess, B.; Lindahl, E. GROMACS: High performance molecular simulations through multi-level parallelism from laptops to supercomputers. *SoftwareX* 2015, *1-2*, 19-25. DOI: 10.1016/j.softx.2015.06.001

(21) Jorgensen, W. L.; Maxwell, D. S.; TiradoRives, J. Development and testing of the OPLS all-atom force field on conformational energetics and properties of organic liquids. *J Am Chem Soc* 1996, *118* (45), 11225-11236. DOI: 10.1021/ja9621760

(22) Jorgensen, W. L.; Tirado-Rives, J. Potential energy functions for atomic-level simulations of water and organic and biomolecular systems. *Proc Natl Acad Sci U S A* 2005, *102* (19), 6665-6670. DOI: 10.1073/pnas.0408037102

(23) Zeron, I. M.; Abascal, J. L. F.; Vega, C. A force field of Li(+), Na(+), K(+), Mg(2+), Ca(2+), Cl(-), and SO(4) (2-) in aqueous solution based on the TIP4P/2005 water model and scaled charges for the ions. *J Chem Phys* 2019, *151* (13), 134504. DOI: 10.1063/1.5121392

(24) Abascal, J. L.; Vega, C. A general purpose model for the condensed phases of water: TIP4P/2005. *J Chem Phys* 2005, *123* (23), 234505. DOI: 10.1063/1.2121687

(25) Doherty, B.; Zhong, X.; Gathiaka, S.; Li, B.; Acevedo, O. Revisiting OPLS Force Field Parameters for Ionic Liquid Simulations. *J Chem Theory Comput* 2017, *13* (12), 6131-6145. DOI: 10.1021/acs.jctc.7b00520

(26) Sambasivarao, S. V.; Acevedo, O. Development of OPLS-AA Force Field Parameters for 68 Unique Ionic Liquids. *J Chem Theory Comput* 2009, *5* (4), 1038-1050. DOI: 10.1021/ct900009a

(27) Geise, G. M.; Park, H. B.; Sagle, A. C.; Freeman, B. D.; McGrath, J. E. Water permeability and water/salt selectivity tradeoff in polymers for desalination. *Journal of Membrane Science* 2011, *369* (1-2), 130-138. DOI: 10.1016/j.memsci.2010.11.054

(28) Zhang, H.; Geise, G. M. Modeling the water permeability and water/salt selectivity tradeoff in polymer membranes. *Journal of Membrane Science* 2016, *520*, 790-800. DOI: 10.1016/j.memsci.2016.08.035

(29) Sata, T.; Yamane, Y.; Matsusaki, K. Preparation and properties of anion exchange membranes having pyridinium or pyridinium derivatives as anion exchange groups. *Journal of Polymer Science Part a-Polymer Chemistry* 1998, *36* (1), 49-58. DOI: 10.1002/(Sici)1099-0518(19980115)36:1<49::Aid-Pola8>3.0.Co;2-X

(30) Sata, T.; Jones, G. N.; Sata, T. *Ion Exchange Membranes: Preparation, Characterization, Modification and Application*; The Royal Society of Chemistry, 2004.

(31) Sagle, A. C.; Ju, H.; Freeman, B. D.; Sharma, M. M. PEG-based hydrogel membrane coatings. *Polymer* 2009, *50* (3), 756-766. DOI: 10.1016/j.polymer.2008.12.019

(32) Jang, E. S.; Kamcev, J.; Kobayashi, K.; Yan, N.; Sujanani, R.; Dilenschneider, T. J.; Park, H. B.; Paul, D. R.; Freeman, B. D. Influence of water content on alkali metal chloride transport in cross-linked Poly(ethylene glycol) diacrylate.2. Ion diffusion. *Polymer* 2020, *192*. DOI: 10.1016/j.polymer.2020.122316

(33) Jang, E. S.; Kamcev, J.; Kobayashi, K.; Yan, N.; Sujanani, R.; Dilenschneider, T. J.; Park, H. B.; Paul, D. R.; Freeman, B. D. Influence of water content on alkali metal chloride transport in cross-linked Poly(ethylene glycol) Diacrylate.1. Ion sorption. *Polymer* 2019, *178*. DOI: 10.1016/j.polymer.2019.121554

(34) Ni, L.; Meng, J. Q.; Geise, G. M.; Zhang, Y. F.; Zhou, J. Water and salt transport properties of zwitterionic polymers film. *Journal of Membrane Science* 2015, *491*, 73-81. DOI: 10.1016/j.memsci.2015.05.030

(35) Ju, H.; McCloskey, B. D.; Sagle, A. C.; Wu, Y. H.; Kusuma, V. A.; Freeman, B. D. Crosslinked poly(ethylene oxide) fouling resistant coating materials for oil/water separation. *Journal of Membrane Science* 2008, *307* (2), 260-267. DOI: 10.1016/j.memsci.2007.09.028

(36) Sagle, A. C.; Van Wagner, E. M.; Ju, H.; McCloskey, B. D.; Freeman, B. D.; Sharma, M. M. PEG-coated reverse osmosis membranes: Desalination properties and fouling resistance. *Journal of Membrane Science* 2009, *340* (1-2), 92-108. DOI: 10.1016/j.memsci.2009.05.013

(37) Wu, Y. H.; Park, H. B.; Kai, T.; Freeman, B. D.; Kalika, D. S. Water uptake, transport and structure characterization in poly(ethylene glycol) diacrylate hydrogels. *Journal of Membrane Science* 2010, *347* (1-2), 197-208. DOI: 10.1016/j.memsci.2009.10.025

(38) Beija, M.; Li, Y.; Lowe, A. B.; Davis, T. P.; Boyer, C. Factors influencing the synthesis and the post-modification of PEGylated pentafluorophenyl acrylate containing copolymers. *European Polymer Journal* 2013, *49* (10), 3060-3071. DOI: 10.1016/j.eurpolymj.2013.05.003

(39) Levitt, M. H. *Spin dynamics: basics of nuclear magnetic resonance*; John Wiley & Sons, 2013.

(40) Nordness, O.; Simoni, L. D.; Stadtherr, M. A.; Brennecke, J. F. Characterization of Aqueous 1-Ethyl-3-Methylimidazolium Ionic Liquids for Calculation of Ion Dissociation. *J Phys Chem B* 2019, *123* (6), 1348-1358. DOI: 10.1021/acs.jpcb.8b11892

(41) Jiang, S.; Sun, H.; Wang, H.; Ladewig, B. P.; Yao, Z. A comprehensive review on the synthesis and applications of ion exchange membranes. *Chemosphere* 2021, *282*, 130817. DOI: 10.1016/j.chemosphere.2021.130817

(42) Henderson, L. J. Concerning the Relationship between the Strength of Acids and Their Capacity to Preserve Neutrality. *American Journal of Physiology-Legacy Content* 1908, *21* (2), 173-179. DOI: 10.1152/ajplegacy.1908.21.2.173

(43) Hasselbalch, K. A. Die Berechnung der Wasserstoffzahl des Blutes aus der freien und gebundenen Kohlensäure desselben, und die Sauerstoffbindung des Blutes als Funktion der Wasserstoffzahl. *Biochemistry. Z* 1917, *78*, 112-144.

(44) Siegel, R. A.; Firestone, B. A. pH-dependent equilibrium swelling properties of hydrophobic polyelectrolyte copolymer gels. *Macromolecules* 2002, *21* (11), 3254-3259. DOI: 10.1021/ma00189a021

(45) Longo, G. S.; de la Cruz, M. O.; Szleifer, I. Non-monotonic swelling of surface grafted hydrogels induced by pH and/or salt concentration. *J Chem Phys* 2014, *141* (12), 124909. DOI: 10.1063/1.4896562

(46) Zofchak, E. S.; Zhang, Z. D.; Marioni, N.; Duncan, T. J.; Sachar, H. S.; Chamseddine, A.; Freeman, B. D.; Ganesan, V. Cation-Ligand Interactions Dictate Salt Partitioning and Diffusivity in Ligand-Functionalized Polymer Membranes. *Macromolecules* 2022, *55* (6), 2260-2270. DOI: 10.1021/acs.macromol.2c00035

(47) Sachar, H. S.; Zofchak, E. S.; Marioni, N.; Zhang, Z. D.; Kadulkar, S.; Duncan, T. J.; Freeman, B. D.; Ganesan, V. Impact of Cation-Ligand Interactions on the Permselectivity of Ligand-Functionalized Polymer Membranes in Single and Mixed Salt Systems. *Macromolecules* 2022, *55* (11), 4821-4831. DOI: 10.1021/acs.macromol.2c00543

(48) Mackie, J. S.; Meares, P. The diffusion of electrolytes in a cation-exchange resin membrane I. Theoretical. *Proceedings of the Royal Society of London. Series A. Mathematical and Physical Sciences* 1997, *232* (1191), 498-509. DOI: 10.1098/rspa.1955.0234

(49) Yasuda, H.; Lamaze, C. E.; Ikenberr.Ld. Permeability of Solutes through Hydrated Polymer Membranes .I. Diffusion of Sodium Chloride. *Makromol Chem* 1968, *118* (Nov), 19-&.

(50) Geise, G. M.; Paul, D. R.; Freeman, B. D. Fundamental water and salt transport properties of polymeric materials. *Progress in Polymer Science* 2014, *39* (1), 1-42. DOI: 10.1016/j.progpolymsci.2013.07.001

(51) Kanduc, M.; Kim, W. K.; Roa, R.; Dzubiella, J. Aqueous Nanoclusters Govern Ion Partitioning in Dense Polymer Membranes. *ACS Nano* 2019, *13* (10), 11224-11234. DOI: 10.1021/acsnano.9b04279

(52) Guilherme, M. R.; Silva, R.; Girotto, E. M.; Rubira, A. F.; Muniz, E. C. Hydrogels based on PAAm network with PNIPAAm included: hydrophilic-hydrophobic transition measured by the partition of Orange II and Methylene Blue in water. *Polymer* 2003, *44* (15), 4213-4219. DOI: 10.1016/S0032-3861(03)00370-7

(53) Delimi, R.; Sandeaux, J.; Gavach, C.; Nikonenko, V. Sorption equilibrium of aromatic anions in an anion exchange membrane. *Journal of Membrane Science* 1997, *134* (2), 181-189. DOI: 10.1016/S0376-7388(97)00104-X

(54) Molina, M. A.; Rivarola, C. R.; Barbero, C. A. Study on partition and release of molecules in superabsorbent thermosensitive nanocomposites. *Polymer* 2012, *53* (2), 445-453. DOI: 10.1016/j.polymer.2011.11.037

(55) Takano, M.; Ogata, K.; Kawauchi, S.; Satoh, M.; Komiyama, J. Ion-specific swelling behavior of poly(N-vinyl-2-pyrrolidone) gel: Correlations with water hydrogen bond and non-freezable water. *Polymer Gels and Networks* 1998, *6* (3-4), 217-232. DOI: 10.1016/S0966-7822(98)00015-X

(56) Yan, N.; Paul, D. R.; Freeman, B. D. Water and ion sorption in a series of cross-linked AMPS/PEGDA hydrogel membranes. *Polymer* 2018, *146*, 196-208. DOI: 10.1016/j.polymer.2018.05.021